

COVER PAGE

Document downloaded by @DAEL

Sat Nov 28 15:01:01 2026
For personal use

When automatic English translation is provided, only the original document is authentic.
The EAA cannot be held responsible of any translation error

Bibliographical reference

Acoustic Effects of Trees Simulated by a Finite-Difference Time-Domain Model, A. Schady, D. Heimann and J. Feng, Acta Acustica **vol. 100** (Number 6), 2014, pp. 1112-1119

DOI
https://doi.org/10.3813/AAA.918790

Acta Acustica united with Acustica
Vol. 100 (2014) 1112 – 1119

DOI 10.3813/AAA.918790

Acoustic Effects of Trees Simulated by a Finite-Difference Time-Domain Model

A. Schady[1)], D. Heimann[1)], J. Feng[2)]

[1)] Deutsches Zentrum für Luft- und Raumfahrt (DLR), Institut für Physik der Atmosphäre, Oberpfaffenhofen, Germany. arthur.schady@dlr.de

[2)] DB Systemtechnik GmbH, Völckerstrasse 5, München, Germany

Summary

The simulation of sound propagation in and around forest areas requires a detailed understanding of the acoustic properties of trees. Therefore, the acoustic properties of laser-scanned real trees and idealized trees are studied by means of a three-dimensional finite difference time domain (FDTD) sound propagation model. The aim is to gain functional relationships between backscattered and transmitted sound pressure levels and selected tree characteristics. The choice of the model type enables the simultaneous consideration of multiple reflections and diffraction of sound waves. The spatial resolution of 5 cm admits a frequency range up to 1350 Hz and the resolution of the trunk and major branches. The simulated sound pressure signals are detected by a virtual microphone array in front and behind an infinitely long row of trees, respectively. Regarding the density of tree material within a volume, thin objects reflect less sound energy than dense objects, which in contrast have a noticeable acoustical effect on the transmission loss. The relations are provided by a set of empirical equations.

PACS no. 43.28.En, 43.50.Rq

1. Introduction

The investigation of the influence of vegetation on sound propagation has a long history (e.g. [1, 2, 3]). There have been contrary statements on how big this influence is, or even if it exists. Makarewicz [4] denies a significant effect of vegetation. On the contrary, Martens and Michelsen [5] show that leaves significantly contribute to sound energy absorption. From recent studies on the influence of single trees, rows of trees or forests it is clear that trees modify the sound field through reflection and scattering of sound wave by trunks, branches and twigs (e.g. [6, 7]). These include theoretical considerations (e.g. scattering by cylinders) [8]. Early studies of sound propagation through vegetation and forests by means of measurement data and model results are described in [9, 10, 11, 12] and more recent study results can be found in [13, 14, 15, 16, 17]. The effects of a single tree were studied by model simulations and quantified by measurements (e.g. [18, 19]) and the effects considering wind and rating the shielding performance of vegetation belts are described in (e.g. [20, 21]). All of these studies describe most of the effects, but they do not provide simplified relationships which can be used to parameterize tree effects in model simulations that cannot resolve single trees in detail, e.g. two-dimensional simulations. Admittedly, the diversity of vegetation on the one hand (such as type, size, shape, density, bark properties) and the variety of acoustic effects on the other hand (e.g. insertion loss depending on density of material, refraction by tree-induced wind modifications, absorption of the bark and the soil, etc.) make it difficult to find such simple relationships. Moreover, one has to distinguish direct and indirect influences of vegetation on sound. Direct effects are caused by parts of the plant above the ground by reflection, scattering and absorption. Indirect effects are due to the modification of the flow field around the plants (e.g. [22]) , or the modification of the acoustical ground properties (e.g. [23]) as they determine refraction or ground attenuation. Finally, the arrangement of an experiment, the type of sound source, the location of the receiver in relation to the studied plants and the measurement procedure play an important role for any judgement about the influence on the sound field. The present study is based on finite difference time domain (FDTD) simulations of the influences of a row of trees on a plane sound wave. The chosen spatial resolution allows to resolve explicitly the tree trunk and major branches in three dimensions. The model is capable of simultaneously simulating multiple reflections and scattering of sound waves. The study aims at deriving functional relationships between tree parameters and their influence on the reflected and transmitted sound scattered by the trees. Tree properties which are associated with the trunk and branches are systematically varied, while the effects of small twigs, leaves or needles had to be disregarded. Indirect tree effects and the effects of the tree size and crown diameter are not considered either.

Received 20 December 2013,
accepted 12 August 2014.

© S. Hirzel Verlag · EAA

In the following we present the model used in this study. Then we describe the trees and the parameterization followed by the simulation setup and the calculation method. Here, the basics of our hypothesis connecting tree parameters with reflection and transmission are derived. In section 3 we present the spatial, the spectral and absorption effects. Finally we propose four equations to determine the amount of reflection and transmission of quantifiable tree properties.

2. Methodology

2.1. Numerical modeling

The three-dimensional finite difference time domain (FDTD) model of sound propagation is based on the linearized Euler equations [24]. Since meteorological effects are not considered in the present paper, the prognostic equations of continuity and momentum simply read

$$\frac{\partial \mathbf{u}}{\partial t} = -\frac{1}{\rho_0}\nabla p, \tag{1}$$

$$\frac{\partial p}{\partial t} = -\kappa p_0 \nabla \boldsymbol{u}. \tag{2}$$

Here, p and $\mathbf{u}$ denote the scalar sound pressure and the particle velocity vector as a function of time t, respectively. The homogeneous background atmosphere is defined by the air density ρ_0 and the air pressure p_0. $\kappa = 1.4$ is the ratio of the specific heats and the sound speed is $c_0 = \sqrt{\kappa p_0/\rho_0}$. This set of equations is solved numerically with a 4th-order spatial differencing scheme by [25], adapted to the staggered C-type grid [26]. The minimum wavelength determining the maximal resolvable frequency in the FDTD model is given by $\lambda_{min} = 5\Delta s$ with the grid spacing $\Delta s = 0.05\,\mathrm{m}$. The ground is implemented as a rigid boundary and the grid cells representing obstacles such as wood are blocked out, i.e. the normal component of $\mathbf{u}$ is set to zero. For the numerical investigation a $L_x = 30$ m long, $L_y = 8\,\mathrm{m}$ wide, and $L_z = 24\,\mathrm{m}$ high model domain was defined. A non-reflecting boundary condition (perfectly matched layer) was applied at the top of the model domain [27]. Cyclic boundary conditions are employed in lateral y-direction such that the domain could be defined as small as possible without a contamination by spurious reflections from the sides. The cyclic boundary condition is equivalent to an infinite row of trees perpendicular to the direction of sound propagation.

2.2. Parameterization of the tree properties

Concerning the diversity of vegetation there are different shapes, sizes and extensions as well as different amounts of plant material within a volume. To find a relationship between tree properties and the effects of trees on sound propagation global parameters suitable for classification are sought. To parameterize the effect of unresolved tree elements (twigs and leaves) in numerical simulations of the turbulent flow through a forest canopy the dimensionless Leaf Area Index (LAI) is often used. It expresses the one-sided green leaf area per unit ground surface area (e.g [28]). The LAI works well in computational fluid dynamics because leafs (and needles) influence the airflow more than trunks and branches. In contrast to airflow, leafs have less relevance in the propagation of sound waves. Instead of LAI, we use parameters which rather characterize the trunk and branches.

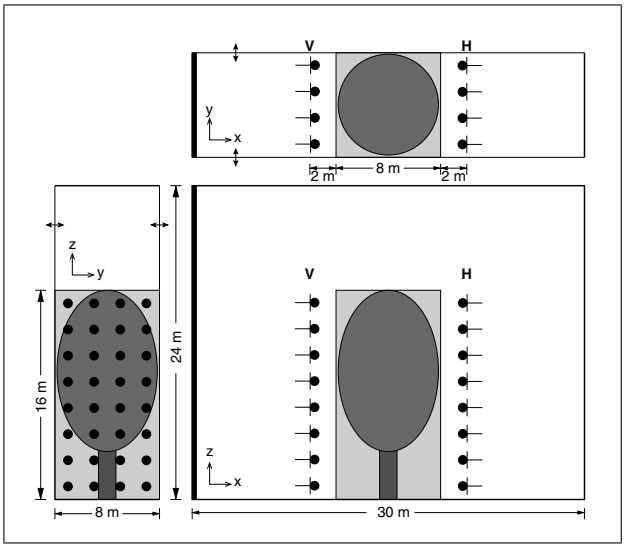

Figure 1. Sketch of the numerical experiment arrangement showing the microphone configuration in the model domain in front and behind the tree and the enveloping volume (shaded).

The parameters used in this study are called "partial volume" (PV) and "partial cross section" (PCS). The partial volume specifies the portion of filled grid cells to all grid cells in the enveloping volume (light grey area in Figure 1), i.e. the relative density of the tree elements. The partial cross section describes the silhouette of the tree on a virtual screen perpendicular to the sound propagation path, i.e. the portion of the screen which is shadowed by the tree. While PV is a general property of a tree, PCS depends obviously on PV as well as on the spatial distribution of the solid tree elements within the volume. Finally, the pathway of a wave through the tree (i. e. the tree size) and the direction of the wave passing the tree determine the PCS. To systematically rate the influence of trees on the sound field two experimental settings are applied: (1) six types of natural (real) trees based on voxel data from laser scans by Bienert *et al.* [29]. The set comprises a single birch tree (*betula pendula*), a single spruce tree (*picea abies*), a clump of three spruce trees, a single oak (*quercus robur*) a real size unscaled tree "plane 2" (*platanus acerifolia*) and the same plane tree with scaled size (height and crown diameter) named "plane 1", (2) six types of idealized though visually realistic trees with prescribed parameters (diameter of trunk d, number of ramifications N_t, number of new branches per ramification N_s) with five random realizations per type (in total 30 cases). These variations result in different PV and PCS numbers, similar to the real trees. The random variations account for the diversity tree within each type. Figure 2 presents

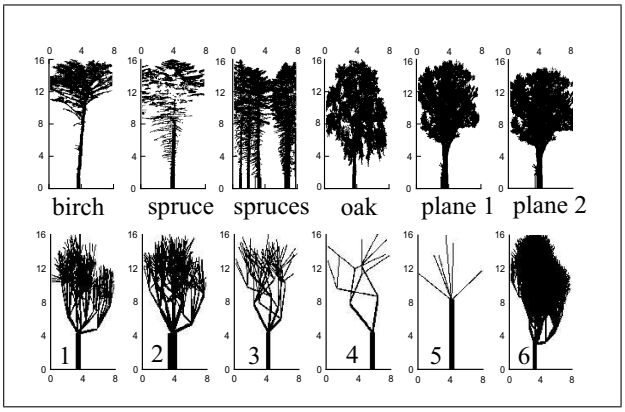

Figure 2. Front view representing the *PCS* of the trees used in this study. In the upper row the laser-scanned trees are shown. In the lower row the front view of the idealized trees is presented, ordered according to the tree type number used for this study.

the shadow relief (*PCS*) of the trees used in this study. The values of *PV* and *PCS* of the real and the idealized trees as well as their influence on the reflected and transmitted sound field are summarized in Table I and II, respectively. Figure 3 visualizes the relationship of *PV* and *PCS* for all objects of this study. The interrelation between *PV* and *PCS* depends on the distribution within the volume, the block size of the elements or the relation of side area ($L_x L_z$ or $L_y L_z$) to total volume ($L_x L_y L_z$).

2.3. Simulation setup

The influence of a single tree on the sound field is examined by comparing a simulation for the undisturbed field without any obstacle to simulations with a scattering object centred in the model domain at $x = 15\,\mathrm{m}$, $y = 4\,\mathrm{m}$. The obstacles inside the model domain have a uniform height of 16 m and a diameter of 8 m. A plane sound wave with the form of a Gaussian pressure pulse with a full width at half maximum $FWHM = 0.125\,\mathrm{m}$, oriented parallel to the y-z-plane, is emitted at the left boundary ($x = 0$) of the model domain and propagates in x-direction towards the obstacle. The pulse represents a distant sound source and incorporates a continuous spectrum of sound waves, with an energy density distribution from 80 dB at $f = 15\,\mathrm{Hz}$ to 50 dB at $f = 1350\,\mathrm{Hz}$. The frequencies up to 1350 Hz are evaluated according to the model resolution. Two arrays of $N = 4 \times 8$ virtual, uniformly distributed receivers in the y-z-plane are located 6 m in front and 6 m behind the centre of the obstacle, i.e. at $x = 9\,\mathrm{m}$ and $x = 21\,\mathrm{m}$. Each receiver k represents a cross-section of $A_k = 4\,\mathrm{m}^2$. At these arrays the backward reflected (index R) and the forward transmitted sound (index T) are recorded, respectively. The cyclic boundary conditions in lateral direction imply that virtually an infinite row of trees is simulated.

The simulation time was chosen to $\tau = 0.088$ s. Within this time the sound pressure pulse propagates through the row of trees where it is partially scattered and reflected into all directions. The simulation time is sufficient to allow

Table I. Parameters *PV* and *PCS* of the laser scanned trees together with the reflection ΔL_R and transmission ΔL_T level.

Tree	*PV* [%]	*PCS* [%]	ΔL_R [dB]	ΔL_T [dB]
Birch	1.39	25.8	−12.2	−0.6
Spruce	0.74	22.7	−13.5	−0.4
3 spruces	2.71	55.6	−6.8	−1.3
Oak	3.37	51.0	−6.5	−1.5
Plane 1	4.71	46.4	−6.4	−1.6
Plane 2	3.98	45.7	−6.9	−1.4

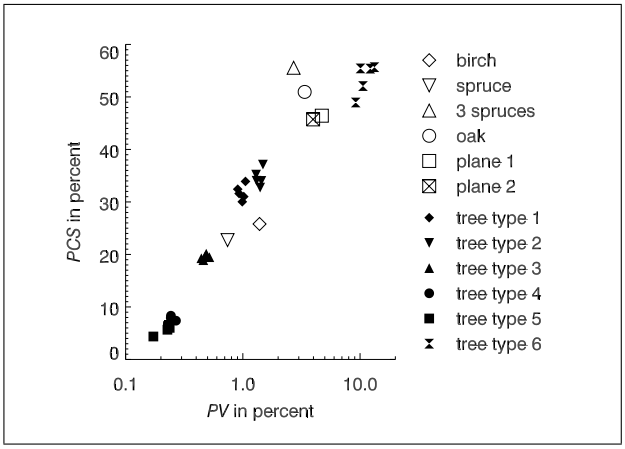

Figure 3. Distribution of tested objects with their relation of partial volume *PV* to partial cross section *PCS*.

sound that is backward/forward scattered at the resolved tree or slantwise scattered at its two immediate neighbours (by the cyclic boundaries) to reach the receiver arrays. Scattered sound from more distant trees cannot reach the receivers within τ anymore. However, this sound would not contribute relevant additional energy to the receivers due to 3-dimensional geometrical spreading.

Figure 4 provides a snapshot of the sound pressure field in the x-z-plane after the pulse has passed the obstacle ($t = 0.065$ s). While the pulse front itself is hardly distorted, irregular patterns around the tree indicate that sound is scattered in all directions. Backward scattered sound waves are counted as reflection and forward scattering or undisturbed propagation as transmission. The incident sound energy does not exactly correspond to the sum of the (forward) transmitted and (backward) reflected sound because of possible losses of upward scattered sound at the absorbing top of the model domain and a small part lost sidewards.

2.4. Calculation method

The influence of the scattering object on the sound field is determined by evaluating the mean acoustic potential-energy density (sound energy per volume) at both receiver arrays for the simulations with and without an object. The acoustic potential-energy density $W_{x,k,sim}$ at a receiver k is

Table II. Parameters PV and PCS of the idealized trees together with the reflection ΔL_R and transmission ΔL_T level.

Number	d [m]	Nt	Ns	PV [%]	PCS [%]	ΔL_R [dB]	ΔL_T [dB]
1	0.5	4	6	0.90 to 1.05	30.0 to 33.9	−9.61 to −9.50	−0.73 to −0.49
2	1.0	4	6	1.30 to 1.48	32.7 to 37.1	−8.89 to −8.70	−0.88 to −0.56
3	0.5	4	4	0.44 to 0.52	18.9 to 20.2	−12.65 to −12.27	−0.40 to −0.26
4	0.5	4	2	0.23 to 0.27	6.5 to 8.3	−17.18 to −15.56	−0.16 to −0.03
5	0.5	2	6	0.17 to 0.24	4.4 to 6.6	−18.68 to −14.86	−0.19 to −0.03
6	0.5	6	6	9.18 to 13.26	48.9 to 55.7	−6.16 to −4.89	−2.84 to −2.26

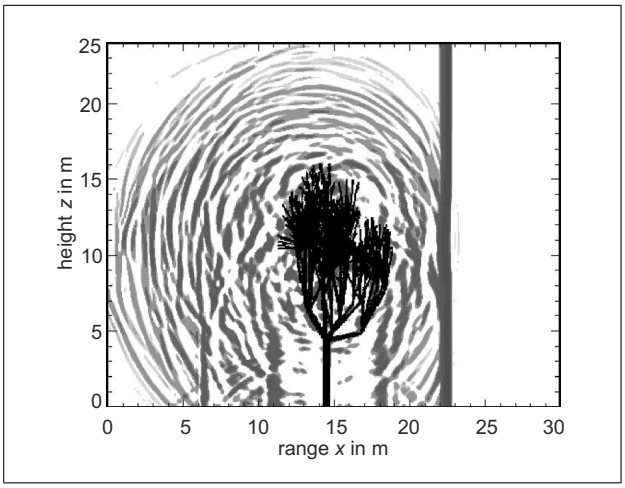

Figure 4. Snapshot of the sound pressure pulse and the scattered sound waves passing the idealized tree type #1. The shades of gray indicate the sound pressure fluctuations normalized to a range from 0 = light to 1 = dark.

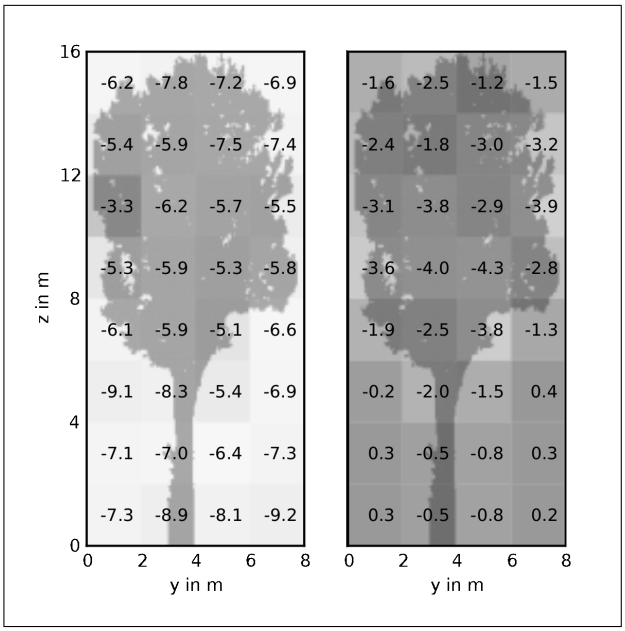

Figure 5. The relative sound level in dB of each virtual microphone in front of (left) and behind (right) the "plane 1" tree relative to the undisturbed case. The represented area of the receivers are shaded in grey scale according to the sound pressure level.

independent of the direction of propagation. It is proportional to the squared time-integrated sound pressure.

$$W_{x,k,sim} = \frac{A_k}{2\rho_0 c_0^2}\frac{1}{\tau}\int_{t=0}^{\tau} p(t)^2_{x,k,sim}\,\mathrm{d}t. \tag{3}$$

The indices are defined as follows: x denotes the positions of the receiver arrays R and T and k indicates a single receiver of an array. The index sim denotes whether it is a simulation with an object (index: $sim = obj$) or without an object (index: $sim = ref$). The mean acoustic potential-energy density at the arrays is then given by

$$W_{x,sim} = \frac{1}{N}\sum_{k=1}^{N} W_{x,k,sim}. \tag{4}$$

For the reference case without an obstacle the sound energy is independent of x and k, i.e. $W_{R,k,ref} = W_{T,k,ref} = W_{k,ref} = W_{ref}$.

We evaluate the energy with the object relative to that without the object. This ration (for convenience expressed as a difference of logarithmic levels) only depends on the squared time-integrated sound pressure since the other terms cancel out. The backward reflected sound energy is then determined by

$$\Delta L_{R,k} = 10\log_{10}\left(\frac{W_{R,k,obj} - W_{k,ref}}{W_{k,ref}}\right),$$
$$\Delta L_R = 10\log_{10}\left(\frac{W_{R,obj} - W_{ref}}{W_{ref}}\right). \tag{5}$$

The transmitted sound energy is determined without subtracting the incoming signal by

$$\Delta L_{T,k} = 10\log_{10}\left(\frac{W_{T,k,obj}}{W_{k,ref}}\right),$$
$$\Delta L_T = 10\log_{10}\left(\frac{W_{T,obj}}{W_{ref}}\right). \tag{6}$$

The relative levels are normally negative because the backward reflected and forward transmitted sound energy are each less than the reference one. However, in the case of focussing, the levels $\Delta L_{x,k}$ can be locally positive. Equation (5) and (6) can be expressed in terms of a fraction γW_{ref} (with $0 \le \gamma \le 1$) of the incident broad band energy and with a free parameter A and B to allow for energy

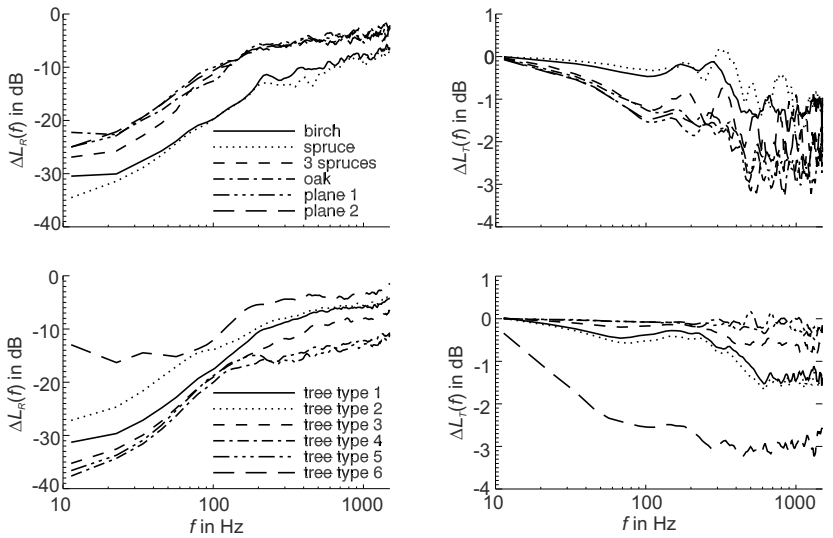

Figure 6. Spectral distribution of reflected (left) and transmitted (right) sound pressure level (SPL). The real trees are presented in the upper panel and the idealized trees in the lower panel.

loss. If this fraction is reflected backwards and exactly the remaining energy $(1-\gamma)W_{ref}$ is transmitted, the result is

$$\Delta L_R = A \log_{10}(\gamma), \tag{7}$$

$$\Delta L_T = B \log_{10}(1-\gamma). \tag{8}$$

Equation (7) and (8) describe the idealized broad band effect of the trees on the specific incident pressure pulse, with A and B being proportionality factors.

3. Model application and results

The results of the simulations are analysed under four aspects: (1) spatial effect of backward reflection and forward transmission, (2) spectral effects, (3) absorption effects and (4) the functional relationship between their influence on the sound and the dependency on the partial volume and cross section.

3.1. Spatial effects

By analysing the spatial effects the influence of tree material distribution on the sound field around the tree becomes obvious. Figure 5 provides $\Delta L_{R,k}$ and $\Delta L_{T,k}$ for the specific pressure pulse and the laser-scanned scaled tree "plane 1". The distributions reveal the inhomogeneity of material within the volume and the 3-dimensional reflection and scattering. It is clear that the crown has a larger effect on broad band sound than the trunk, i.e. more sound energy is reflected or backscattered (larger ΔL_R) and less is transmitted (smaller ΔL_T) in the crown layer. Note that the cyclic boundary condition in y-direction implies a row of trees so that neighbouring trees also contribute to the shown distributions. Although there are spatial effects, the bulk effect of the trees across the receiver arrays is considered in the following sections.

3.2. Spectral effects

Spectral effects are caused by the varying ratio of the length scales of the scattering and reflecting objects and the wavelength of the involved frequency of the impinging sound pressure pulse. Figure 6 illustrates the spectral effects caused by the tree elements. It shows the spectral compositions of ΔL_R (right-hand panels) and ΔL_T (left-hand panels) for the real trees and the idealized trees. The spectra are evaluated by performing fast Fourier transforms on the recorded sound pressure time signal at the receivers. They indicate that low-frequency sound (<200 Hz) is almost not directed backward and passes the trees without significant attenuation. Differences in the curves are a consequence of the different parameters PV and PCS of the single trees. The effect of density (PV) on reflection is to observe in the upper left panel. Here the thin trees i.e. birch and spruce reflect much less sound energy over the total frequency range than the other trees. The idealized trees show this characteristics (e.g. tree type #3, #4 and #5) as well. Regarding transmission (the right panels) the signal of idealized tree type #6 differs clearly from the others. The PCS numbers of tree type #6 (i.e. 48.9 to 55.7), is similar to the PCS numbers of the clump of three spruces (55.6) or the PCS numbers of the oak tree (51.0). Nevertheless, the transmission through tree type #6 is much more attenuated (cf. ΔL_T values in Tables I and II). The probable reason is the high PV value of this type of tree.

3.3. Absorption effects

Pioneering work concerning absorption of tree bark was done by Reethof [30]. The general conclusion was that the absorption coefficients of six tested species are quite low and largely independent of frequency. We used the relation between the absorption coefficient α and the reflection coefficient β according to $\alpha = 1 - \beta$ and performed a study with a variable reflection coefficient β of the solid elements

within the volume by assuming that branches and other non-leafy structures behave like real impedances. Due to multiple reflections it could be possible that energy loss is not linear with the magnitude of the reflection coefficient. Our simulations indicate that a decreased reflection coefficient causes an energy loss in the propagating sound waves reaching the microphones before and behind the obstacle.

The effect is illustratively shown for tree type #1 in Figure 7. As the reflection coefficient β is lowered from 1 to 0.5, ΔL_R decreases from -10 dB to -15 dB and ΔL_T decreases from 0.6 dB to 1 dB.

3.4. Empirical equations

For the purpose of parameterizing the acoustical effects of a tree, a functional relationship between one or more parameters describing the character of the tree and its acoustical effect is sought. The following prerequisites should be fulfilled: (a) For a given tree the parameter must be determinable in practice. (b) The functional relationship must be distinct.

Starting from equations (7) and (8), we simply assume that the fraction γ of energy that is backscattered or transmitted depends on the partial volume PV or the partial cross section PCS.

We assume

$$\gamma = rPV^m \tag{9}$$

and

$$\gamma = sPCS^l. \tag{10}$$

This assumption ensures a fraction $\gamma = 0$ in the absence of a tree ($PV = PCS = 0$), i.e. no reflection and a complete transmission. For $r = 1$ and $s = 1$ the assumption implies that $\gamma = 1$ in the case of completely dense ($PV = PCS = 1$) and seamlessly placed trees, i.e. a complete reflection and no transmission. If the geometry allows for sound propagation (e.g. by diffraction or diffuse reflection) around and over the trees, the factors r and s may deviate from unity even for $PV = PCS = 1$ to allow for $0 < \gamma < 1$. Inserting equations (9) and (10) into (7) and (8) leads to

$$\Delta L_R = c_{1,R,PV} \log_{10}\left(PV\right) + c_{2,R,PV}, \tag{11}$$

$$\Delta L_R = c_{1,R,PCS} \log_{10}\left(PCS\right) + c_{2,R,PCS}, \tag{12}$$

$$\Delta L_T = c_{1,T,PV} \log_{10}\left(1 - c_{2,T,PV} PV^{c_{3,T,PV}}\right), \tag{13}$$

$$\Delta L_T = c_{1,T,PCS} \log_{10}\left(1 - c_{2,T,PCS} PCS^{c_{3,T,PSC}}\right). \tag{14}$$

The coefficients c_x in equations (11) to (14) are determined by curve fitting separately for backward reflection / scattering (index R) and forward transmission (index T), each with the partial volume (PV) and the partial cross section (PCS) as independent variables. The curve-fitting algorithm uses the gradient-expansion method to compute non-linear least squares fits. The fitted coefficients for calculation of ΔL_R and ΔL_T (in dB) are provided in Table III together with the root mean square error ($RMSE$). They refer to a reflection coefficient $\beta = 1$. In Figure 8a the functional relationship of $\Delta L_R(PV)$ for all simulated objects indicates that PV is a good parameter to describe reflection. The sparse trees like birch and spruce (with a partial volume around 1%) reflect much less sound energy (-12 dB) than the dense trees like the plane or the oak (-7 dB). The fitted curve that is valid for the range of $0.1\% \leq PV \leq 20\%$ confirms the hypothesis that the reflection depends on PV. The simplified approach according to equation (7) with $A = 5.6$ leads to a $RMSE = 1.5$ dB.

Figure 8b shows the functional relationship of $\Delta L_T(PV)$ according to equation (13). The dense trees like tree type #6 ($PV \approx 10\%$) or the oak (PV=3.4%) lead to a high insertion loss behind the tree of about 2 dB due to their acoustical shadowing effect. Sound transmis-

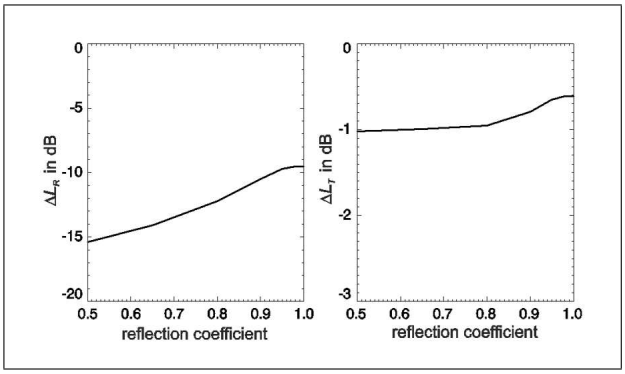

Figure 7. The backwards scattered sound energy (left) and the transmitted sound energy (right) depending on the reflection coefficient β, here calculated for the idealized tree type #1.

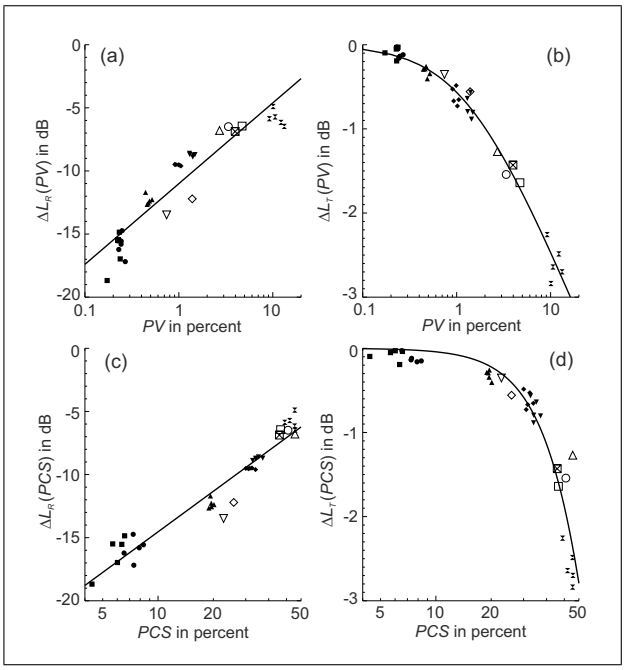

Figure 8. Scatter diagrams together with the fitted curves according to adequate equations: a) $\Delta L_R(PV)$ and equation (11); b) $\Delta L_T(PV)$ and equation (13) ; c) $\Delta L_R(PCS)$ and equation (12) and d) $\Delta L_T(PCS)$ and equation (14). The coefficients from Table III were used and the symbols representing the trees are as in Figure 3.

Table III. Coefficients from curve fitting for equations (11) to (14) and the *RMSE*.

Effect	$c_{1,y,x}$	$c_{2,y,x}$	$c_{3,y,x}$	*RMSE* [dB]
$\Delta L_R(PV)$	6.39	1.78		1.41
$\Delta L_R(PCS)$	10.68	−3.86		0.98
$\Delta L_T(PV)$	−2.40	−130.6	1.13	0.11
$\Delta L_T(PCS)$	−22.4	−1.15	2.43	0.27

sion through a tree with PV <1% is nearly undisturbed ($\Delta L_T \approx 0$). The regression results in a very low *RMSE* compared to the regression for $\Delta L_R(PV)$. However, the sensitivity of the parameters $c_{2,T,PV}$ and $c_{3,T,PV}$ in equation (13) remains problematic.

For simplified approximation one could use equations (7) and (8). In both cases, i.e. reflection and transmission, the dependency on PV is evident. But, PCS depends additionally on the pathway of the sound wave passing an obstacle. Therefore it seems to be more realistic, using PCS as the parameter for the regression while PV is implicitly included. Additionally PCS could be estimated by simply analysing a photo of a tree. Even so, the regression results do not reveal a big difference between using PV or PCS (see Table III). In Figure 8c the model results $\Delta L_R(PCS)$ are plotted. The magnitude of backscattered sound corresponds similarly to PV also to the PCS of the trees. The curve fitting for $\Delta L_R(PCS)$ gives a better estimation with a $RMSE = 0.98$ dB compared to $\Delta L_R(PV)$. Similarly Figure 8d shows the functional relationship between transmission effect and the PCS (i.e. $\Delta L_T(PCS)$). Here the fitting is slightly worse than for $\Delta L_T(PV)$ but is still good.

4. Discussion and conclusions

We developed a structured numerical experiment to study the effect of a row of trees on the acoustic field around them and to quantify their effect of reflection and transmission depending on determinable parameters like the partial volume (PV) and the partial cross section (PCS) of the tree. The presented simulations show a clear interrelation between the acoustic effect of trees and the tree density. This was checked more profoundly by applying idealized trees of adjustable parameters and comparing their influence on the sound field with laser scans of real trees. All parameters as well as the effects of the idealized trees correspond very well to those of the real trees. There were derived a set of equations with empirical parameters to calculate the reflection and transmission effect of the scattering objects. The parameters in equation (11) to (14) include all the effects like ground reflection, absorption by tree bark, microphone distance and arrangement, wind effects, the pathway through (i.e. the size of) the tree as well as the typical size of the blocking elements. Even if recent work showed that scattering from real trees in-situ is influenced by the state of the ground near the tree, we modelled here a rigid soil. The limitations of this study are due to the demand to keep the experiment simple and clear. For a better comparability of the trees it was suitable to scale all objects to a standardized enveloping volume. The scaling does not change the relation between PV and PCS value of a tree. Nevertheless our approach is a general guess of the magnitude of sound reflection and transmission for a plane sound pressure pulse by a porous medium like a tree.

Acknowledgement

We like to thank very much Mrs. A. Bienert for providing the data of the laser scanned trees in high resolution. Furthermore, the authors thank all the proof readers for their critical remarks.

References

[1] C. F. Eyring: Jungle acoustics. Journal of the Acoustical Society of America **18** (1946) 257–270.

[2] T. F. W. Embleton: Sound Propagation in Homogeneous Deciduous and Evergreen Woods. Journal of the Acoustical Society of America **35** (1963) 796.

[3] D. Aylor: Noise reduction by vegetation and ground. Journal of the Acoustical Society of America **51** (1972) 197–205.

[4] R. Makarewicz: Phenomenology of sound-propagation through a green belt. Journal of Sound and Vibration **72** (1980) 481–489.

[5] M. Martens, A. Michelsen: Absorption of Acoustic Energy by Plant-Leaves. Journal of the Acoustical Society of America **69** (1981) 303–306.

[6] D. Heimann: Numerical Simulations of wind and sound propagation through an idealised stand of trees. Acta Acustica united with Acustica **89** (2003) 779–788.

[7] J. M. Wunderli, E. M. Salomons: A Model to Predict the Sound Reflection from Forests. Acta Acustica united with Acustica **95** (2009) 76–85.

[8] V. Twersky: Multiple scattering of waves by a volume distribution of parallel cylinders. Journal of the Acoustical Society of America **36** (1964) 1314–1329.

[9] R. Bullen, F. Fricke: Sound propagation through vegetation. Journal of Sound and Vibration **80** (1982) 11–23.

[10] W. Leschnik: Zur Schallausbreitung in bebauten und bepflanzten Gebieten. Acustica **44** (1980) 14–22.

[11] F. Fricke: Sound-attenuation in Forests. Journal of Sound and Vibration **92** (1984) 149–158.

[12] A. Pal, V. Kumar, N. Saxena: Noise attenuation by green belts. Journal of Sound and Vibration **234** (2000) 149–165.

[13] A. Tunick: Calculating the micrometeorological influences on the speed of sound through the atmosphere in forests. Journal of the Acoustical Society of America **114** (2003) 1796–1806.

[14] M. E. Swearingen, M. J. White, P. J. Guertin, D. G. Albert, A. Tunick: Influence of a forest edge on acoustical propagation: Experimental results. Journal of the Acoustical Society of America **133** (2013) 2566–2575.

[15] C. Fang, D. Ling: Investigation of the noise reduction provided by tree belts. Landscape and Urban Planning **63** (2003) 187–195.

[16] C. Fang, D. Ling: Guidance for noise reduction provided by tree belts. Landscape and Urban Planning **71** (2005) 29–34.

[17] A. Tunick: Numerical experiment to revisit micrometeorology and sound speed calculations in forests. Meteorology and Atmospheric Physics **107** (2010) 103–108.

[18] M. Hornikx, D. Botteldooren, T. Van Renterghem, J. Forssén: Modelling of scattering of sound from trees by the pstd method. Forum Acusticum, Aalborg, Denmark, pp. 6. (2011).

[19] H.-S. Yang, J. Kang, C. Cheal, T. V. Renterghem, D. Botteldooren: Quantifying scattered sound energy from a single tree by means of reverberation time. Journal of the Acoustical Society of America **134** (2013) 264–274.

[20] T. Van Renterghem, D. Botteldooren, K. Verheyen: Road traffic noise shielding by vegetation belts of limited depth. Journal of Sound and Vibration **331** (2012) 2404–2425.

[21] T. Van Renterghem, D. Botteldooren: Numerical simulation of the effect of trees on downwind noise barrier performance. Acta Acustica united with Acustica **89** (2003) 764–778.

[22] G. Gross: Numerical simulation of canopy flows. Springer Verlag Heidelberg, 1993.

[23] K. Attenborough: Review of ground effects on outdoor sound propagation from continuous broadband sources. Applied Acoustics **24** (1988) 289 – 319.

[24] R. Blumrich, D. Heimann: A linearized eulerian sound propagation model for studies of complex meteorological effects. Journal of the Acoustical Society of America **112** (2002) 446–455.

[25] C. K. W. Tam, J. C. Webb: Dispersion-relation-preserving finite difference schemes for computational acoustics. Journal of Computational Physics **107** (1993) 262–281.

[26] A. Arakawa, V. Lamb: Computational design of the basic dynamical processes of the ucla general circulation model. Methods in Computational Physics **17** (1977) 173–265.

[27] J.-P. Berenger: A perfectly matched layer for the absorption of electromagnetic waves. Journal of Computational Physics **114** (1994) 185–200.

[28] F. Hosoi, K. Omasa: Voxel-based 3-d modeling of individual trees for estimating leaf area density using high-resolution portable scanning lidar. Geoscience and Remote Sensing, IEEE Transactions on **44** (2006) 3610 –3618.

[29] A. Bienert, R. Queck, A. Schmidt, C. Bernhofer, H.-G. Maas: Voxel space analysis of terrestrial laser scans in forests for wind field modelling. IAPRS **XXXVIII** (2010) 92–97.

[30] G. Reethof, O. McDaniel, G. Heisler: Sound absorption characteristics of tree bark and forest floor. in Heisler, Gordon M.; Herrington, Lee P., eds. Proceedings of the conference on metropolitan physical environment; Gen. Tech. Rep. NE-25. Upper Darby, PA: U.S. Department of Agriculture, Forest Service, Northeastern Forest Experiment Station. (1977) 206 –217.